Materials Letters 183 (2016) 34–39

Contents lists available at ScienceDirect

Materials Letters

journal homepage: www.elsevier.com/locate/matlet

Subgrain formation in ultrasonic enhanced friction stir welding of aluminium alloy

G.K. Padhy, C.S. Wu *, S. Gao

MOE Key Lab for Liquid-Solid Structure Evolution and Materials Processing, and Institute of Materials Joining, Shandong University, Jinan, 250061 China

ARTICLE INFO

Article history:
Received 29 January 2016
Received in revised form
3 June 2016
Accepted 9 July 2016
Available online 9 July 2016

Keywords:
Friction stir welding
Microstructure
Recrystallization
Subgrain
Ultrasonic

ABSTRACT

Recrystallization fractions in the stirred zone of Al 6061-T6 friction stir welds, prepared with and without ultrasonic vibrations, were evaluated using recrystallization fraction maps. Based on the maps, it was suggested that the microstructure evolution can be described as different dislocation manipulation processes. It was observed that superposition of static load of FSW on residual ultrasonic softening induces subgrain formation. Subgrain formation was substantial at the center of the stirred zone where the ultrasonic impact was the maximum.

1. Introduction

Current understanding on the microstructure evolution in friction stir welding (FSW) is largely qualitative and inadequate to establish a fundamental science [1]. Recently, ultrasonic vibration enhanced FSW (UVeFSW) has been developed to economically extend the FSW process to harder materials [2]. As compared to FSW, the UVeFSW of aluminium (Al) alloys resulted with lower process load, improved material flow, wider deformation zone, and better weld physical and mechanical properties [2,3]. Besides, the UVeFSWed Al 6061-T6 alloy comprised of better grain refinement, recrystallization, grain orientation, and strain characteristics [3,4]. The above improvements were attributed to the more favourable dislocation dynamics achieved in the UVeFSW. Therefore, UVeFSW has the potential for the economic welding of harder alloys.

In UVeFSW, the FSW process load is superimposed on the ultrasonic effect. Previous studies predicted that the ultrasonic effect is maximum in the weld center and diminished towards the stirred zone extremities (SZE) [3,4]. Superposition of ultrasonic vibrations on static load causes ultrasonic softening [5,6] of material which alters the physical, mechanical and metallurgical properties of the material [7–11]. Ultrasonic softening is described by the reduction in quasi-static stress due to stress superposition, i.e., augmentation of quasi-static load with the oscillatory stress of ultrasound [12]. In micro-indentation studies of Al-alloy, stress superposition resulted with extensive subgrain formation [7,13]. This was attributed to reduction in dislocation density due to increasing chances of dislocation annihilation. Subgrains facilitate metal deformation by reducing the number of local active slip systems [14]. Withdrawal of ultrasonic vibrations reduces the ultrasonic softening to residual softening [4,12]. Most of the ultrasonic studies considered only the surface frictional effects on the plastic deformation while the volumetric effects were neglected.

Ultrasonic irradiation produces recovered grains in metal [15]. Hence, a workpiece in UVeFSW consists of recovered grains rather than coarse grains before the welding. The higher deformation in UVeFSW was attributed to an enhanced material flow velocity which indicates reduction in flow stress by ultrasonic vibrations [16,17]. Also, the higher deformation would cause internal crystal rotations which alter the subsequent dislocation generation and recrystallization. In this study, the effect of ultrasonic vibrations on the recrystallization of Al-alloy in UVeFSW was evaluated using local recrystallization fraction (RF) maps. The RF maps were derived from electron backscattered diffraction (EBSD) based data on internal average misorientation (IAM) of individual grains.

2. Materials and methods

Single pass welds of 6 mm thick Al 6061-T6 plates were prepared using FSW and UVeFSW processes under identical process

* Corresponding author.
E-mail address: wucs@sdu.edu.cn (C.S. Wu).

http://dx.doi.org/10.1016/j.matlet.2016.07.033
0167-577X/

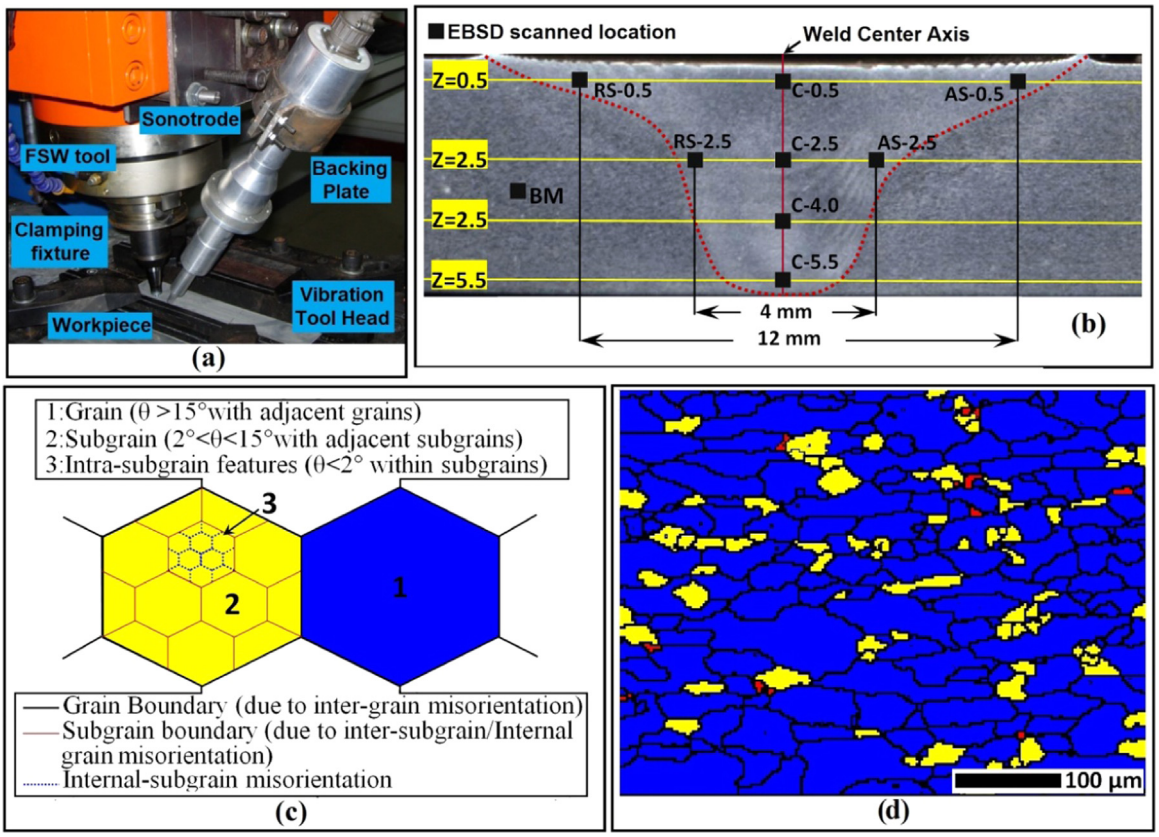

Fig. 1. (a) Photograph of UVeFSW, Schematics of (b) SZ locations scanned by EBSD (c) grain, subgrain and internal subgrain features, (d) RF map of base metal.

parameters (rotation speed 800 rpm, welding speed 320 mm/min, shoulder plunge depth 0.05 mm, and tool tilt angle 2.5°). The FSW machine was position-control type. FSW tool comprised of a concave concentric shoulder (diameter 15 mm) and a threaded pin (diameter ~3.5–6 mm and length ~5.75 mm). Fig. 1a shows the UVeFSW setup. In UVeFSW, ultrasonic vibration was imparted at 45° by the tool head of the sonotrode (fixed to FSW machine) along the weld seam line of workpiece. The tool head was moved 20 mm ahead of the FSW tool. The sonotrode was operated at a frequency, 20 kHz, amplitude, 40 μm, normal load, 300 N and has an output power, 300 W. Details of the UVeFSW is provided elsewhere [18].

Fig. 1b shows the transverse SZ locations selected for EBSD scanning. The locations are at depths Z=0.5, 2.5, 4.0 and 5.5 mm along the weld center axis (WCA) and at depths Z=0.5 and 2.5 mm on the advancing side (AS) and retreating side (RS) of the SZ extremities (SZE). EBSD scanning was conducted using a scanning electron microscope (ZeissEvoMA 10) equipped with an EBSD (NordlysMax II detector and *HKL* CHANNEL5 Tango data-processing module). Parameters used for the scanning were step size 0.5 μm, low-angle boundary (LAB) 2° and high-angle boundary (HAB) 15°. The Tango module generated the RF maps automatically by first constructing the grains on the basis of the pre-established HAB and later by calculating the IAM inside each grain. Subsequently, a grain with IAM >2° (generally, ~4–5°) was classified as deformed grain (DG) while that without LABs and with IAM <2° was classified as recrystallized grain (RG). A substructured grain (SG) comprised of subgrains with IAM <2° and inter-subgrain misorientation >2°. Fig. 1c shows the grain, subgrain and inter-subgrain features. Percentages of DG, RG and SG in the RF maps were evaluated on the basis of grain area.

3. Results and discussion

The UVeFSW process is different from other stress superposition processes. Considering the linear kinematics of FSW tool and ultrasonic tool head during welding, the material undergoing UVeFSW can be described to be under an integrated effect of quasi-static load superimposed on residual softening. This is because, at each instance of welding, the moving tool head generates a residual softening which is augmented by the load of the following FSW tool. In UVeFSW, the initial dislocation generation by ultrasonic irradiation increases the dislocation motion. The improved dislocation motion facilitates dislocation consumption which makes deformation of material easier during the action of FSW tool. Subsequently, at the beginning of microstructure evolution, dislocations are regenerated, rearranged or re-consumed depending upon the heat generation, mechanical stress, strain etc. Therefore, in this study, RF analysis has been carried out by assuming the microstructure evolution as a series of dislocation manipulation phenomena. The internal dislocation density of a grain varies directly as its IAM. For example, Fig. 1d shows the RF map of Al 6061-T6 base metal where grains are ~94% recrystallized, ~5% substructured and <1% deformed. Accordingly, the base metal has ~93% HAB (represents RG) and ~7% LAB (represents SG) [3].

Figs. 2 and 3 show the RF maps of the locations in WCA and SZE, respectively. Fig. 4 shows the stacking of RG, SG and DG percentages, calculated from Figs. 2 and 3. The RF maps in Fig. 2a show that C-0.5 locations in both FSW and UVeFSW are dominated by SGs. This may be attributed to slower microstructure evolutions due to recurring shoulder effect. The recurring effect arises from the different sizes of the shoulder and the location and allows multiple shoulder rotations on C-0.5 resulting with relatively slower overall dislocation consumption. Fig. 4a shows that the RG:

Please cite this article as: G.K. Padhy, et al., Subgrain formation in ultrasonic enhanced friction stir welding of aluminium alloy, Mater Lett (2016), http://dx.doi.org/10.1016/j.matlet.2016.07.033

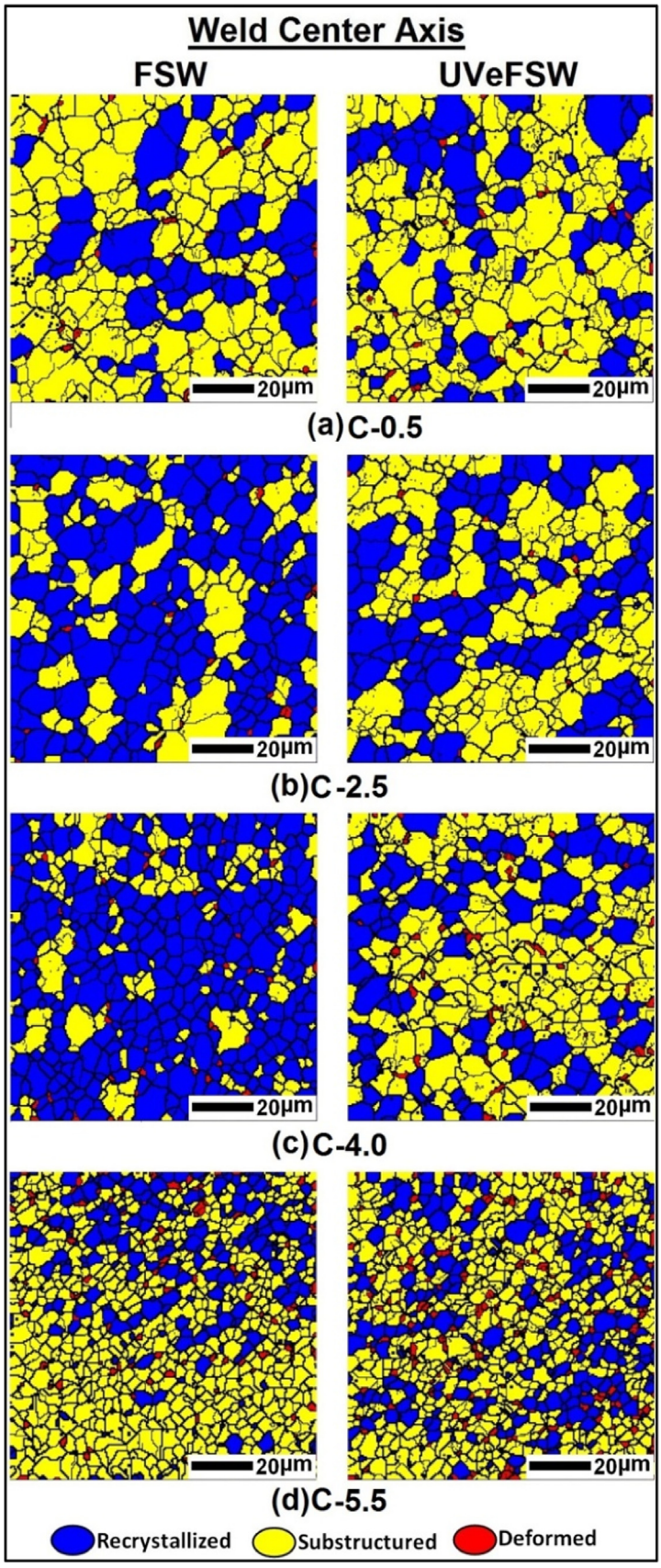

Fig. 2. RF maps of WCA.

Please cite this article as: G.K. Padhy, et al., Subgrain formation in ultrasonic enhanced friction stir welding of aluminium alloy, Mater Lett (2016), http://dx.doi.org/10.1016/j.matlet.2016.07.033

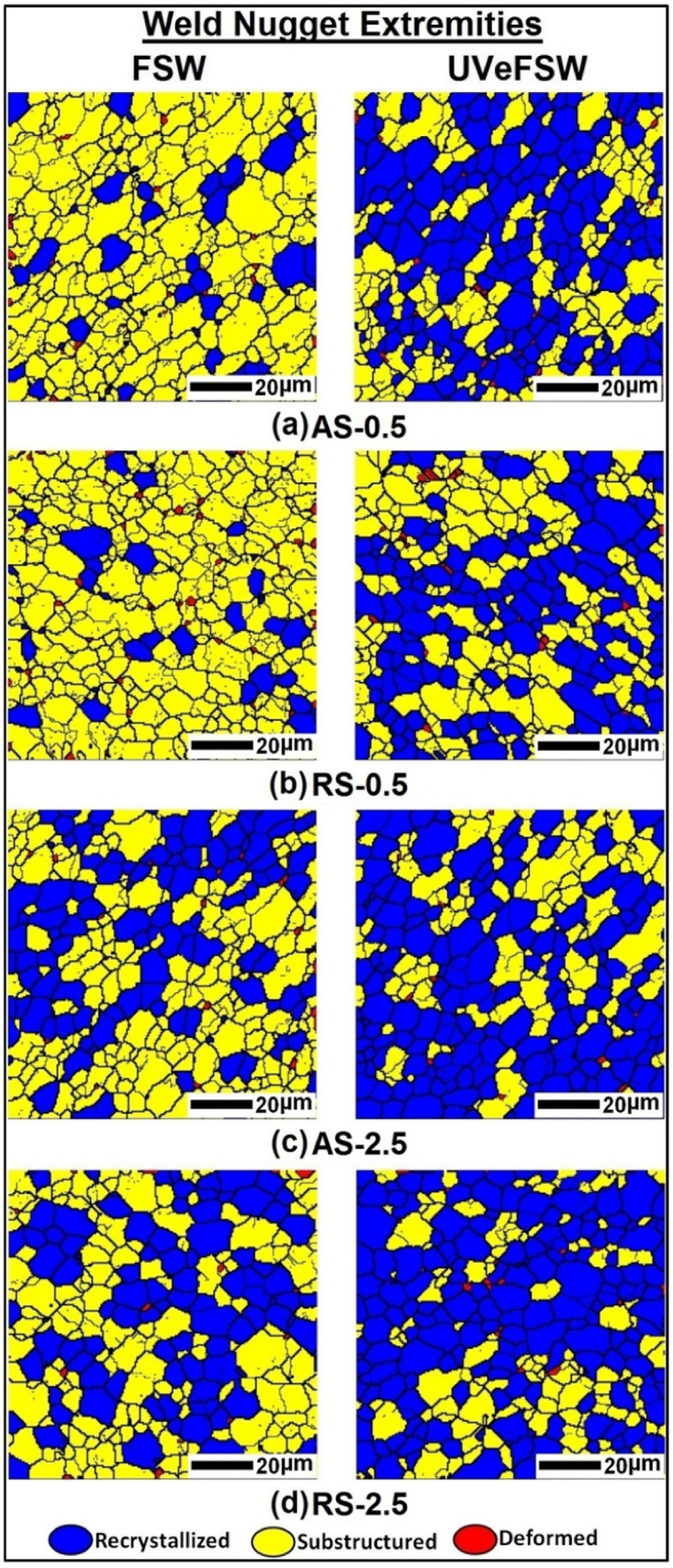

Fig. 3. RF maps of SZE.

Please cite this article as: G.K. Padhy, et al., Subgrain formation in ultrasonic enhanced friction stir welding of aluminium alloy, Mater Lett (2016), http://dx.doi.org/10.1016/j.matlet.2016.07.033

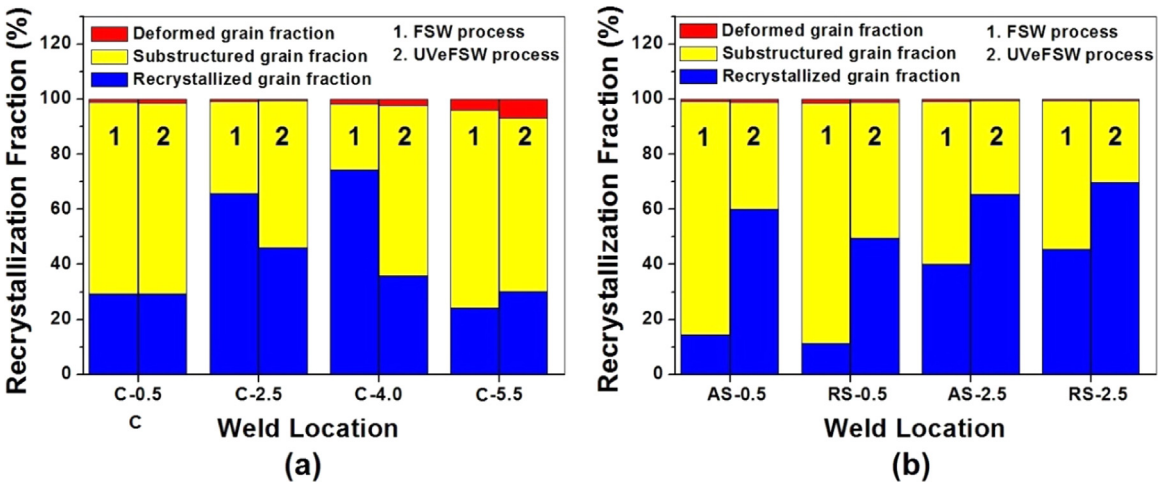

Fig. 4. RF in FSW and UVeFSW (a) along WCA, (b) at SZE.

SG:DG at C-0.5 are similar in both FSW and UVeFSW with ~24% RG, 75% SG and ~1% DG. This indicates that the ultrasonic effect is not significant at C-0.5. The higher degree of subgrain formation can be attributed to thermal softening of material which causes dislocation consumption. This leads to variation in IAM values favourable for transformation of the initially deformed structure into SGs. Interestingly, C-2.5 in UVeFSW has equal proportions of RG and SG while that in FSW is clearly dominated by RGs, i.e., lower internal dislocation density (Fig. 2b). Fig. 4a clarifies that %SG in UVeFSW is higher (~53%) than that in FSW (~34%). Similarly, C-4.0 in FSW has RG dominance while that in UVeFSW is substantially dominated by SG (Fig. 2c). Fig. 4a shows that SG in UVeFSW (~64%) is much higher than that in FSW (~26%). Also, the %SG at C-4.0 is marginally higher than that at C-2.5 in UVeFSW. Earlier studies predicted that ultrasonic effect during UVeFSW is significant at C-2.5 and C-4.0 [3] and ultrasonic superimposition on static load causes subgrain formation [7,13]. Therefore, the higher %SGs at C-2.5 and C-4.0 in UVeFSW can be attributed to the superposition of the quasi-static load of FSW tool on the localized residual softening. The stress superposition causes regeneration, consumption and rearrangement of dislocations to produce favourable dislocation localization for SG formation. DGs in both the processes are $<1\%$ at C-2.5 and $<2\%$ at C-4.0. The higher %DG and %SG at N-4.0 than at C-2.5 indicate that a higher degree of thermal softening acts simultaneously with the residual softening towards the subgrain formation at C-4.0. At C-5.5 (Fig. 2d), %(SG+DG) is very high (~70–75%) and similar in both the processes (Fig. 4a). The high %SG can be attributed to thermal softening effects due to very high heat generation at the tool pin tip [3] while the similar %SG is due to insignificant ultrasonic effect at C-5.5 [5,6]. From a dislocation viewpoint, the residual softening is significant at C-2.5 and C-4.0. Therefore, the microstructure evolution in UVeFSW at these locations begins with very high dislocation densities and ends at moderately high dislocation densities despite the gradual dislocation consumption during microstructure evolution. This condition favours subgrain formation. At C-0.5 and C-5.5, the recrystallization is completely thermal driven.

Fig. 3 shows that AS-0.5 (Fig. 3a), RS-0.5 (Fig. 3b), AS-2.5 (Fig. 3c) and RS-2.5 (Fig. 3d) of FSW are highly substructured while those in UVeFSW have RG dominance. The RG:SG:DG histograms of SZE (Fig. 4b) show that the %SG at AS-0.5 and RS-0.5 are ~86% each in FSW while those in UVeFSW are ~40% and ~50% respectively. DG is $<1\%$ in both the processes. The %SG at AS-2.5 and RS-2.5 are reduced to ~60% each in FSW and to ~30% and 34%, respectively in UVeFSW. In the SZE locations, the %SG are higher at Z=0.5 mm than at Z=2.5 mm for both processes. It is known that the subgrain formation can be triggered by both ultrasonic vibrations and heat [7,19]. Given the insignificant ultrasonic effect at SZE [3], the higher %SG in FSW indicates that the thermal plasticity experienced by the SZE in FSW is much higher than that in UVeFSW. This further indicates that microstructure evolution processes along the horizontal lines at each depth of the SZ are interdependent. The interdependence retards the dislocation consumption in the SZE of FSW more than that in UVeFSW. The slower dislocation consumption leads to higher internal dislocation density in grains which makes the IAM favourable for subgrain formation.

Apart from the subgrain formation in the center of SZ, the ultrasonic vibrations also induce reduction in grain size, as observed in a recent study [3]. However, the grain sizes of similar SZE locations of FSW and UVeFSW are the same. This confirms that the differences in subgrain formation in the SZE are due to the interdependency of microstructure evolution processes along the horizontal lines of SZ. Some earlier investigations based on ultrasonic upsetting and bonding/consolidation experiments [15] suggested that upper and lower parts of the joints experience the maximum ultrasonic effect. However, the extensive subgrain formation in the SZ center of UVeFSW shows that ultrasonic impact is significant in the center.

4. Conclusion

Variations in the recrystallized, substructured and deformed fractions of WCA and SZE locations infer that the recrystallization processes vary at different locations of SZ in both FSW and UVeFSW. The microstructure evolution process in FSW can be interpreted in terms of dislocation manipulation processes. Microstructure in the SZ of FSW is dominated by substructured grains except for the weld center while that in the UVeFSW has substructured grains along WCA and recrystallized grains at SZE. Ultrasonic induced subgrain formation in UVeFSW is prominent in the locations where the ultrasonic impact is significant. Superposition of quasi-static load of FSW tool on residual softening by ultrasonic irradiation is sufficient to induce subgrain formation in UVeFSW.

Acknowledgement

Authors acknowledge the financial supports of National Natural Science Foundation of China (Grant Nos. 51550110501 and

Please cite this article as: G.K. Padhy, et al., Subgrain formation in ultrasonic enhanced friction stir welding of aluminium alloy, Mater Lett (2016), http://dx.doi.org/10.1016/j.matlet.2016.07.033

51475272) and China/Shandong University International Postdoctoral Exchange Program.

References

[1] U.F.H.R. Suhuddin, S. Mironov, Y.S. Sato, H. Kokawa, Mater. Sci. Eng. A 527 (2010) 1962–1969.
[2] G.K. Padhy, C.S. Wu, S. Gao, Sci. Technol. Weld. Join. 20 (2015) 631–649.
[3] G.K. Padhy, C.S. Wu, S. Gao, L. Shi, Mater. Des. 92 (2016) 710–723.
[4] S. Gao, C.S. Wu, G.K. Padhy, L. Shi, Mater. Des. 99 (2016) 135–144.
[5] A. Rusinko, Ultrasonics 51 (2011) 709–714.
[6] Z. Yao, G.Y. Kim, Z. Wang, L.A. Faidley, Q. Zou, D. Mei, Z. Chen, Int. J. Plast. 39 (2012) 75–87.
[7] K.W. Siu, A.H.W. Ngan, I.P. Jones, Int. J. Plast. 27 (2011) 788–800.
[8] S. Bagherzadeh, K. Abrinia, Q. Han, Mater. Lett; 10.1016/j.matlet.2016.01.095.
[9] Y. Daud, M. Lucas, Z. Huang, J. Mater. Proc. Technol. 186 (2007) 179–190.
[10] Y. Liu, S. Suslov, Q. Han, C. Xu, L. Hua, Mater. Lett. 67 (2012) 52–55.
[11] X. Chen, J. Yan, S. Ren, J. Wei, Q. Wang, Mater. Lett. 95 (2013) 197–200.
[12] A. Siddiq, T.E. Sayed, Mater. Lett. 65 (2011) 356–359.
[13] K.W. Siu, A.H.W. Ngan, Philos. Mag. 91 (2001) 4367–4387.
[14] R. Sedlacek, W. Blum, J. Kratochvil, S. Forest, Metall. Mater. Trans. A 33A (2002) 319–327.
[15] E. Mariani, E. Ghassemieh, Acta Mater. 58 (2010) 2492–2503.
[16] X.C. Liu, C.S. Wu, G.K. Padhy, Sci. Technol. Weld. Join. 20 (2015) 345–352.
[17] X.C. Liu, C.S. Wu, G.K. Padhy, Scr. Mater. 102 (2015) 95–98.
[18] L. Shi, C.S. Wu, X.C. Liu, J. Mater. Process Technol. 222 (2015) 91–102.
[19] S.K. Sahu, A. Navrotsky, High Temperature Materials and Mechanisms, CRC Press,, Florida 2014, pp. 17–38.

Please cite this article as: G.K. Padhy, et al., Subgrain formation in ultrasonic enhanced friction stir welding of aluminium alloy, Mater Lett (2016), http://dx.doi.org/10.1016/j.matlet.2016.07.033